Journal of Sustainability Science and Management
Volume 19 Number 8, August 2024: 39-48
eISSN: 2672-7226

PERIODICITY OF A DISCRETE STANDARD MAP ON 3-DIMENSIONAL LATTICE

SALEH MOHAMMAD HANIF AND WAN ROZALI WAN NUR FAIRUZ ALWANI*

Dynamical Systems and Their Applications Research Unit, Department of Computational and Theoretical Sciences, Kulliyyah of Science, International Islamic University Malaysia, Bandar Indera Mahkota Campus, Jalan Sultan Ahmad Shah, 25200 Kuantan, Pahang, Malaysia.

**Corresponding author: fairuz_wnfawr@iium.edu.my*
http://doi.org/10.46754/jssm.2024.08.004
Received: 1 August 2023 *Accepted: 8 May 2024* *Published: 15 August 2024*

Abstract: The study of resonances of Hamiltonian systems with a divided phase space is a well-established area of research which attracted the interests of many researchers over the years. One can study such resonances over a discrete space. This paper focuses on the rotational motion of the orbits in the 3-dimensional lattice, Z^3. We construct discrete maps from 2-dimensional to 3-dimensional. We consider the transformations that give periodicity to the 3-dimensional space. On a specific value of initial conditions and parameters alpha and beta, the orbit of the 3-dimensional map is periodic while the rest are non-periodic. Some observations on the reduction from a 3-dimensional map to a 2-dimensional by using principal component analysis (PCA) are investigated analytically in this paper.

Keywords: Hamiltonian systems, nonlinear rotations, arithmetic dynamics, rotations in 3 dimensional space, sustainable periodicity.

Introduction

Researchers have been investigating Hamiltonian systems with discrete phase space for many years. Discretisation has been used for a variety of purposes since Rannou's pioneering work (Rannou, 1974), including simulating quantum effects in classical systems, fulfilling invertibility in a delicate numerical experiment, arithmetically illustrating Hamiltonian chaos, and researching various phenomena related to numerical orbits.

The Chirikov-Taylor standard map has received much attention in the cylinder phase space (Chirikov & Shepelyansky, 2008).

Definition 1: (Chirikov-Taylor Standard Map)

The Chirikov-Taylor standard map is defined by

$$\Gamma: T^2 \to T^2$$

such that

$$P_{n+1} = P_n + k \sin q_n,$$
$$q_{n+1} = q_n + P_{n+1}, \quad (1)$$

where, $T^2 = (\mathrm{R}/\mathrm{Z})^2$ *is the torus, k is the perturbation parameter with a value of* $0 < k < 1$*, P_n represents momentum and q_n is the angle formed by the kicked rotor.*

In our scenario, we wish to create a discrete version of the standard map (Chirikov & Shepelyansky, 2008) in Definition 1. We want to investigate the Chirikov-Taylor standard map's discrete version and how the points' dynamics behave in discrete space. The dynamics of the discrete space differ from the dynamics of the cylinder phase space. However, its discrete version features some similarities, especially in the construction of the island chains, as illustrated in Figure 1. This paper provides a basic overview of rotations in 2-dimensional and 3-dimensional discrete spaces.

Definition 2: (Discrete Chirikov-Taylor Standard Map)

On a doubly periodic square lattice $(Z/NZ)^2$*, the discrete form of the Chirikov-Taylor standard map in (1) is defined as follows:*

$\gamma : (Z/NZ)^2 \rightarrow (Z/NZ)^2$, *such that*

$\{yt + 1 \equiv yt + V(xt) \ (mod\ N)$, *where* (2) $x_{t+1} \equiv x_t + y_{t+1} \ (mod\ N)$,

$$V(x) = \begin{cases} +1, & 0 \le x < \lfloor \frac{N}{2} \rfloor, \\ -1, & \lfloor \frac{N}{2} \rfloor \le x < N, \end{cases} \quad (3)$$

is the discrete map's perturbation function and N is a huge fixed integer representing the lattice's size.

Zhang and Vivaldi (1998), constructed the equation in (2).

We constructed the discrete phase space shown in Figure 1 from (2). In Figure 1, island chains of odd order are filled with periodic points. Then, on one of the islands, we construct a local mapping to investigate the behaviour of the points.

Definition 3: (Local Mapping)

The local mapping on one of the islands is given by (Zhang & Vivaldi, 1998),

$$\varphi : Z^2 \rightarrow Z^2, \quad \text{where}$$
$$Y_{n+1} = Y_n - sign(X_n),$$
$$X_{n+1} = X_n + \alpha Y_{n+1} + \beta, \quad \text{with} \quad (4)$$
$$\alpha \ge 1, \quad 0 \le \beta < \alpha \quad \text{and}$$
$$sign\ (X) = \begin{cases} +1, & if\ X \ge 0, \\ -1, & if\ X < 0. \end{cases}$$

Here, α and β are the non-negative parameters.

Figures 2 (A) and 2 (B) depict the orbit of the map specified in (4).

The behaviour of the discrete points φ defined in (4) is thoroughly studied in the research on "Nonlinear rotations on a lattice" by

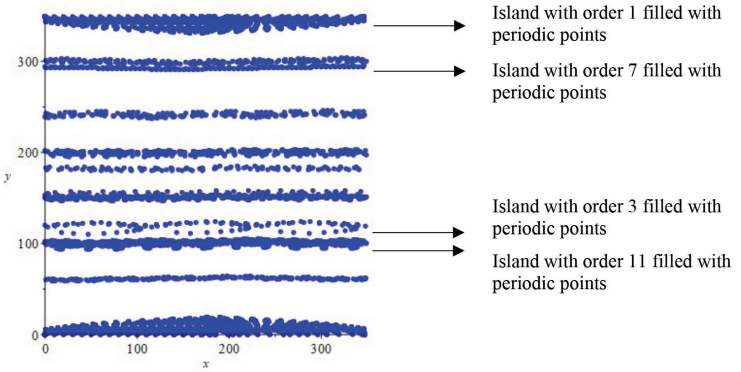

Figure 1: Figure shows the phase diagram in a doubly periodic lattice. There are the discrete orbits of the map (2) with $N = 350$, and $V(x)$ given by (3)

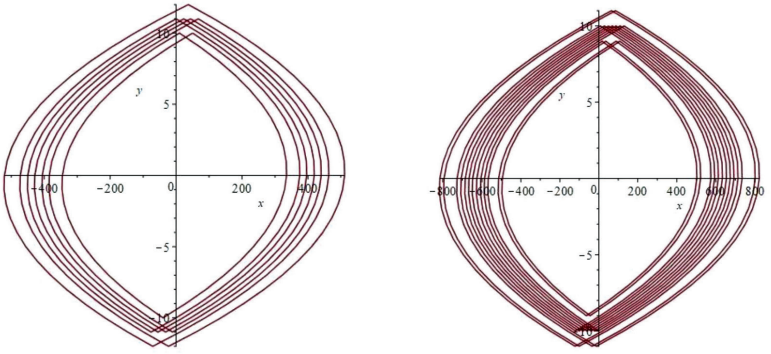

A: The orbit of φ for α = 7, β = 1. B: The orbit of φ for α = 13, β = 2.

Figure 2: Elliptic-type orbits of the local mapping defined in (4)

Alwani and Vivaldi (2018). They have proved the following theorem:

Theorem 1

Let φ be the local mapping defined in ***Definition 3*** *and let* $\hat{\alpha} = \frac{\alpha}{gcd(\alpha, 2\beta)}$.

The period of the orbit φ does not exceed $\hat{\alpha}$. *Furthermore, for any sufficiently large initial condition values, all orbits have period* $\hat{\alpha}$. *They have also proved that if* $\hat{\alpha}$ *is even (or divisible by 4), all orbits will ultimately approach infinity and escape in both directions.*

In this paper, we will look at the behaviour of the orbit of the discrete map specified in (4), which will be defined in a 3-dimensional discrete space, Z^3. 3D modelling produces a 3-dimensional object using 3-dimensional modelling software (Ghani *et al*., 2019).

This approach is used in multimedia and animation to model a figure to animate and in film studies. Characters, whether in novels, films, or games, are among the most crucial aspects to remember when creating media that people can relate to (Bailey, 2013). 3D is often used in medicine to pinpoint the root of an issue (Beane, 2012). Architects utilise 3D software in conjunction with CAD programmes to design models and test and visualise those models to see what structures might look like in photos before they are built (Beane, 2012). The usage of 3D imagination is widespread, and it is continually evolving. The 3D hypothetical is utilised in the animation, creative multimedia, engineering, and medical industries (Luan *et al*., 2008).

From our perspective, two perpendicular axes exist in 2-dimensional space: The horizontal *x*-axis and the vertical *y*-axis. The *z*-axis, which is perpendicular to both the *x* and *y*-axes, can be added as a third dimension. This is referred to as the 3-dimensional space, which reflects the three dimensions that we experience in everyday life.

The purpose of visualising in 3-dimensional space is to aid in comprehending and studying specific behaviours and difficulties. Dynamical systems may be found in ecology, electronics, non-linear mechanics, fluid dynamics, mathematics, economics, and other fields (Haramburu & Delrieux, 2006). Most of the time, these systems cannot be solved in closed form. As a result, they can only be completely comprehended using graphical methods in 3-dimensional space.

Different ways of acquiring, processing, and visualising 3D information from photographs have been investigated, mostly for distant purposes. The key benefits of image-based modelling over laser scanners are that the sensors are typically less costly and portable and that 3D information may be retrieved properly regardless of the size of the item (Remondino & El-Hakim, 2006). In addition to the demonstration of principles, we are inspired by the magnificent 3-dimensional architectures of odd chaotic attractors (Lucas & Sander, 2022). This describes how 3D printing can create genuine physical models of such dynamical systems in practice.

In this topic, we are interested in studying the structure of the discrete map defined in **Definition 2** from a 2-dimensional map into a 3-dimensional map. Alwani and Vivaldi (2018) have reduced the 2-dimensional into a 1-dimensional map by using the Poincaré surface of the section. However, in our case, we consider the 2-dimensional map to be viewed in the 3-dimensional map to observe the different structures of the 2-dimensional map that are periodic in the 3-dimensional map. What are the possible conditions of the *z*-axis so that the rotations are closed and complete its orbit?

This 3-dimensional map is then reduced to the 2-dimensional map by the principal component analysis (PCA) method to compare its 2-dimensional structure with the original 2 dimensions. The method of dimension reduction is discussed in the next section. Most equations defined in *z*-axis are not periodic, which means that the orbits of the map are not closed.

In this paper, we will consider two cases. Case 1 is about the modification of the 2-dimensional discrete Chirikov-Taylor map

defined in (4) into the 3-dimensional version and Case 2 is about the special case obtained from the modification of the 2-dimensional to 3-dimensional map ("twisted" plane). In these two 3-dimensional cases, we want to reduce the dimension using PCA and investigate their orbits in the 2-dimensional space.

Principal Component Analysis

This paper will consider the principal component analysis (PCA). PCA is commonly used to decrease the dimensionality of a set of 3-dimensional data to 2-dimensional coordinates. PCA has been used effectively on movement data as a feature extractor as well as a data-driven filter (Daffertshofer *et al.,* 2004). Its significance for the (clinical) research of human movement sciences (e.g., diagnostics and intervention assessment) is obvious but mostly unexplored. PCA aims to find the most relevant basis for re-expressing a given data set (Kurita, 2019).

This new foundation is designed to expose latent structures in the data set and filter out noise. Dimensionality reduction, data compression, feature extraction, and data visualisation are only examples of uses.

The main advantages of PCA are its low noise sensitivity, lower capacity and memory needs, and enhanced efficiency due to the smaller dimensions of the processes (Karamizadeh *et al.*, 2013). Other advantages of PCA are lack of data redundancy due to orthogonal components (Asadi *et al.*, 2010), reduced complexity of picture grouping, smaller database representation since only the trainee pictures are retained on a reduced basis in the form of their projections, and noise reduction since the maximum variation basis is used and hence tiny fluctuations in the background are disregarded automatically.

PCA is also a statistical approach for detecting patterns in high-dimensional data and representing data with fewer variables (or dimensions) while maintaining as much variability as feasible. In order to reduce the dimensionality of a set of 3D coordinates into 2D coordinates using PCA, a few steps must be computed which include centring the data, computing the covariance matrix, computing the eigenvectors and eigenvalues of the covariance matrix, projecting the data onto the principal components, and normalising the data. The generated 2D coordinates will retain as much variety as feasible from the original 3D data. This can be beneficial for data visualisation activities requiring lower-dimensional data representations.

We perform the PCA in this study using Google Colaboratory (Google Colab). Through a Jupyter Notebook interface, it is intended to facilitate data analysis, machine learning, deep learning, and other data-related activities. A few steps need to be completed to investigate our PCA result. We extract the list of orbits from Maple software and convert them into points. Then, we apply the Google Colab to run and execute the PCA since we want to reduce the dimension of the map through PCA. Through PCA, we can preserve distance and variation between the data points. In this case, after reducing the 3-dimensional case, we want to compare whether the reduced PCA map is the same as the 2-dimensional map defined in (4).

The reduction of 3D to 2D is done through the process which is shown in the following flow chart in Figure 3.

The Modification of 2-dimensional Discrete Space Defined in (4) to 3-dimensional Discrete Space

We are interested in studying the dynamics of our original 2-dimensional map defined in (4) when viewed in a 3-dimensional map. Is it possible to attain the periodicity of the orbit of φ defined in 3-dimensional? We consider cases where the periodicity of the orbit is sustained. From the original 2-dimensional map defined in (4), we construct the 3-dimensional map by adding and modifying the z-axis. What happens to the XY-plane of the map defined in (4) if it is adjusted by "lifting" the XY-plane by 45° from the horizontal plane? Thus, we have the following:

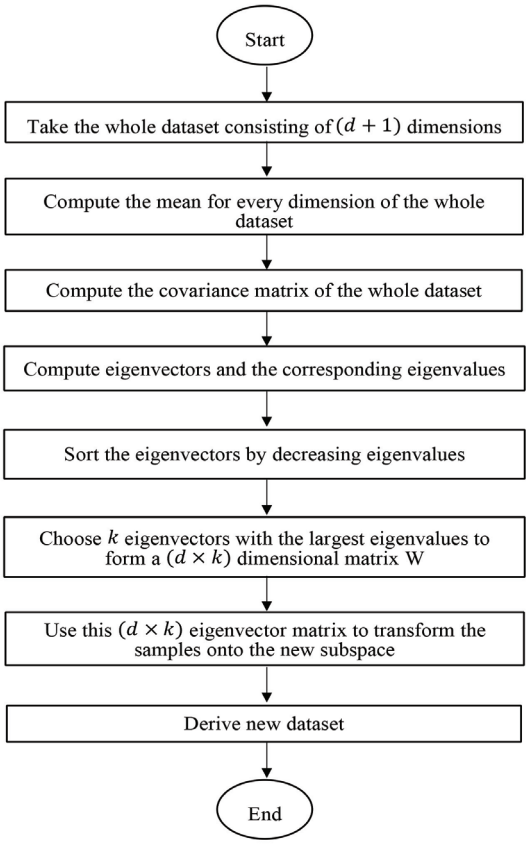

Figure 3: Flow chart of the reduction of 3D to 2D

$$\psi: Z^3 \to Z^3,$$
$$Y_{n+1} = Y_n - sign(X_n), \quad (5)$$
$$X_{n+1} = X_n + \alpha Y_{n+1} + \beta,$$
$$Z_{n+1} = Z_n - sign(X_n),$$

where $\alpha \geq 1$, $0 \leq \beta < \alpha$ and

$$sign(X) = \begin{cases} +1, if\ X \geq 0, \\ -1, if\ X < 0. \end{cases}$$

From (5), we let $(X_0, Y_0, Z_0) \in Z$ be the initial condition and the iterations, $(X_1, Y_1, Z_1) \ldots (X_n, Y_n, Z_n)$ under the mapping of ψ be the points of the orbit of the map defined in (5). Some observations on the orbit of ψ in 3-dimensional space are shown in Figures 4, 5, and 6.

In Figure 6, one can see that the *YZ-plane* is on an angle of 45° from the horizontal axis. We plot the above graph (Figure 6) in the 2-dimensional map and one has that,

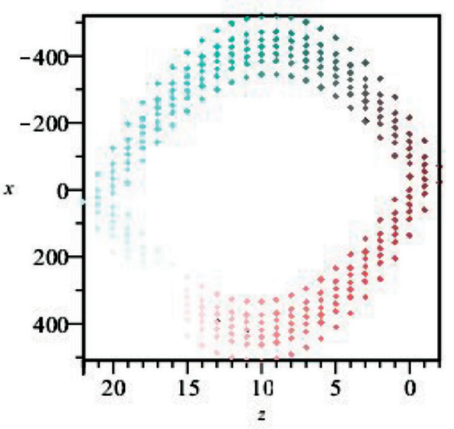

Figure 4: Figure shows the orbit of ψ from *Y*-orientation

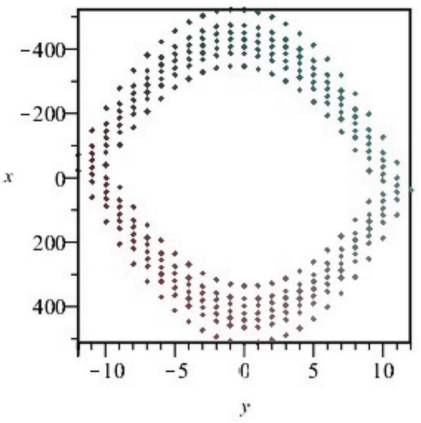

Figure 5: Figure shows the orbit of ψ from Z-orientation

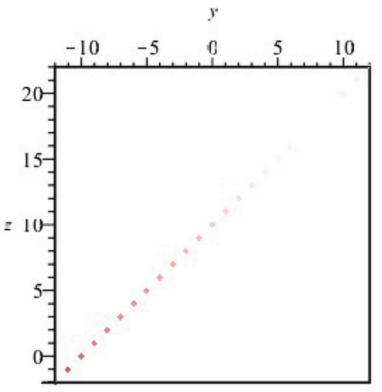

Figure 6: Figure shows the side view of the *YZ-plane* (or view from the orientation of the *x*-axis)

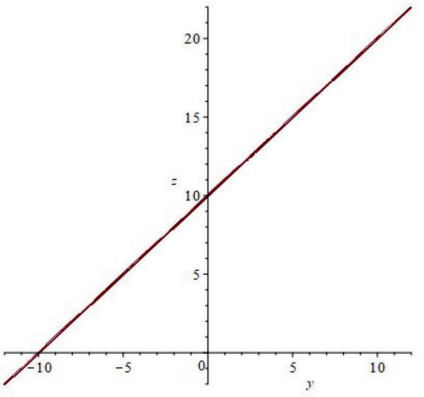

Figure 7: Figure shows the 2-dimensional map of ψ in the *YZ-plane*

We have the following:

Lemma 1: *Let ψ be the 3-dimensional map defined in (5) and let $(y_n, z_n) \in Z$ and $(y_0, z_0) \in Z$ be two points in the orbit of the YZ-plane where $y, z \in Z$. Thus, from the projection on the $X-$ axis, the angle of the "tilted" plane is given by*

$$tan\ \theta = \frac{|z_n - z_0|}{|y_n - y_0|} = 1,\ where\ \theta = 45°$$

Proof. Let (Y_n, Z_n) and (Y_{n+1}, Z_{n+1}) be two points in the orbit defined in (5). From equation Y_{n+1} and Z_{n+1} in (5), we have the following,

$$tan\ \theta = \frac{|Z_{n+1} - Z_n|}{|Y_{n+1} - Y_n|} \quad \frac{|-sign(X_n)|}{|-sign(X_n)|} == 1$$

This [illegible] hus, $\theta = 45°$.

In (5), one can see that the equation for Y_n and Z_n have the same form. The only difference between Y_{n+1} and Z_{n+1} is the initial coordinate (Y_0, Z_0). We let $Y_0 \neq Z_0$, this means that $Y_{n+1} \neq Z_{n+1}$. For $\alpha = 7$ and $\beta = 1$, we have the following figure:

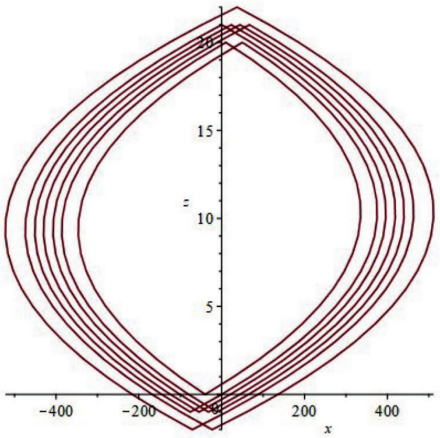

Figure 8: Figure shows that the orbit of ψ on the *XY-plane* for $\alpha = 7, \beta = 1$. The trajectory of the orbits revolves around the centre (a single point) $\hat{\alpha}$ times

By comparing the orbit of the discrete map ψ on the *XZ-plane* defined in (4), and the 3-dimensional map ψ defined on the *XZ-plane*, one can see that the orbits of the map in (4) look

similar to the orbits of ψ in (5) with different orientation as shown in Figure 8. From Figures 4, 5, and 6, we have plotted the graph to see how the orbits of ψ formed in 3-dimensional space.

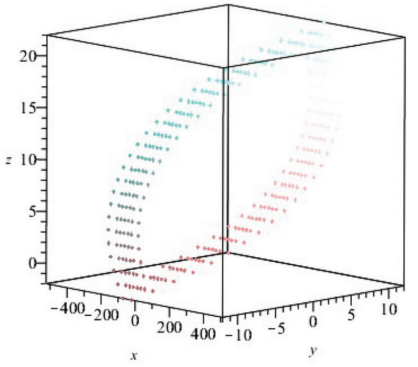

Figure 9: Figure shows the 3-dimensional orbit of ψ

From (5), the orbit of ψ formed a "tilted" plane of X and Y in the 3-dimensional space. The equations of Y_n and Z_n of the mapping

$$\psi: Z^3 \rightarrow Z^3,$$

are quite similar (which gives a value of a constant). Specifically, if the initial condition (X_0, Y_0, Z_0) where $Y_0 \neq Z_0$, then for any values of $(X_0, Y_0, Z_0) \in Z^3$, the next iteration of the point, say Y_1 and Z_1, they will decrease by a single point.

Therefore, if $Y_0 = Z_0$, this means that the equations of Y_n and Z_n in the orbit of ψ will be the same. Thus, one can define the following:

$$\begin{aligned} \rho: \mathbb{Z}^2 &\rightarrow \mathbb{Z}^2, \\ Z_{n+1} &= Z_n - sign(X_n), \\ Xn{+}1 &= Xn + \alpha Zn{+}1 + \beta. \end{aligned} \tag{6}$$

By equalising the equations Y_n and Z_n, we reduce the map defined in (5) into 2-dimensional space. Thus, by letting $\alpha = 7, \beta = 1$, we obtain the following diagram.

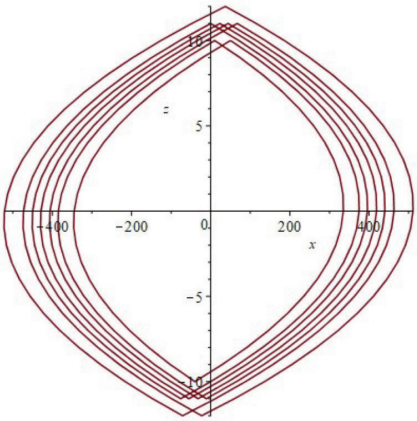

Figure 10: The figure shows the orbit of ψ on the *XY-plane* for $\alpha = 7, \beta = 1$, from the initial condition of $Y_0 = Z_0$

Next, we want to consider the principal component analysis (PCA) for this case to compare whether the result that we will get for *XY*-plane is the same as the periodic result that we got in (5). After completing the PCA process, we have the following visualisation.

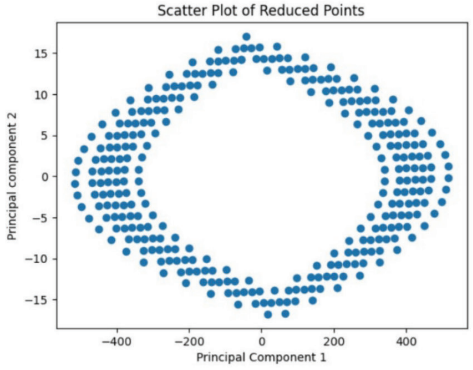

A: PCA visualisation of ψ

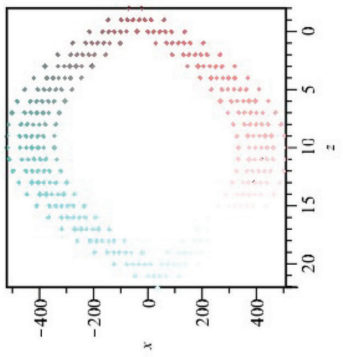

B: The orbit of ψ

Figure 11: Figure shows the diagram A: PCA visualisation of ψ on the *XY-plane* and the orbit of ψ from *Y*-orientation for $\alpha = 7, \beta = 1$

From Figure 11, one can see that the orbit of ψ defined in (5) has the same form as the orbit of PCA visualisation. If we look at the periodicity of these two maps, the period of the orbit is the same which is

$$\hat{\alpha} = \frac{\alpha}{\gcd(\alpha, 2\beta)} = \frac{7}{\gcd(7,2)} = 7.$$

This means that the orbit rotates around its centre point 7 times and closes its orbit (periodic) as we can view it in the above diagram in Figures 10 (A) and 10 (B).

The Special Case ("twisted" plane)

Again, for this special case, we construct the 3-dimensional map by the same method as explained in Case 1. From (4), we define the mapping as follows:

$$\begin{aligned} \omega: \mathbb{Z}^3 &\to \mathbb{Z}^3, \\ Y_{n+1} &= Y_n - sign(X_n), \\ X_{n+1} &= X_n + \alpha Y_{n+1} + \beta, \end{aligned} \tag{7}$$

$$Zn{+}1 = XnYn + sign(Zn)\alpha - \beta - Yn{+}1 + Xn{+}1,$$

where $\alpha \geq 1, \quad 0 \leq \beta < \alpha,$ and

$$sign\,(X) = \begin{cases} +1, if\ X \geq 0, \\ -1, if\ X < 0, \end{cases} \quad \text{and}$$

$$sign\,(Z) = \begin{cases} +1, if\ Z \geq 0, \\ -1, if\ Z < 0. \end{cases}$$

We observe that if we let ω be the map defined in (7) be the 3-dimensional map, and if

$$\hat{\alpha} = \frac{\alpha}{\gcd(\alpha, 2\beta)},$$

then, for some initial conditions $(X_0, Y_0, Z_0) \in Z^3$, the orbit of ω defined in (7) is periodic with period $\hat{\alpha}$ in the 3-dimensional lattice. We have the following diagram:

In Figure 12, the orbit of the map ω described in the equation of Z in (7) features the same trajectory as seen in Figure 2 (A) due to the orientation of the z-axis. The map is plotted on the XY-plane, and in this instance, the periodicity of the map ω in (7) can be checked.

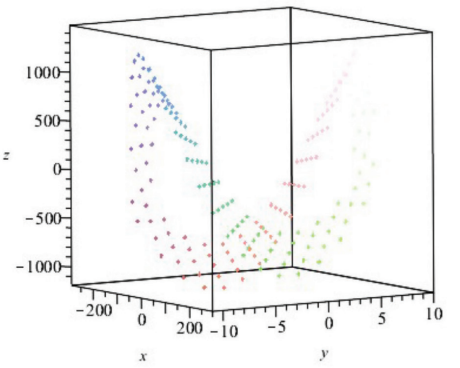

Figure 12: Figure shows the trajectory of the orbit of ψ defined in (7) for $\alpha = 5, \beta = 2$

On the other hand, the map ω shows different orbit trajectories, as illustrated in Figures 12 and 13.

In Figure 13, the original *XY-plane* on the original 2-dimensional map φ defined in (4) looks "twisted".

In Figure 14, one can see that the orbit of ω revolves around its centre (middle points intersection) $\hat{\alpha} = 5$ times. The plane shown in Figures 12 and 13 however is not "twisted" if we view the 3-dimensional map (Figure 12) from above or the *XY-plane*.

As a result, for some initial conditions, the orbits of the 3-dimensional map ω described in (7) are periodic. Case 2's behaviour is very interesting to investigate. For some initial conditions, as demonstrated in the computational

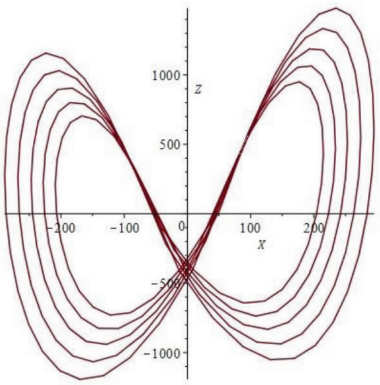

Figure 13: Figure shows the orbit of ψ which is plotted on the *XY-plane*

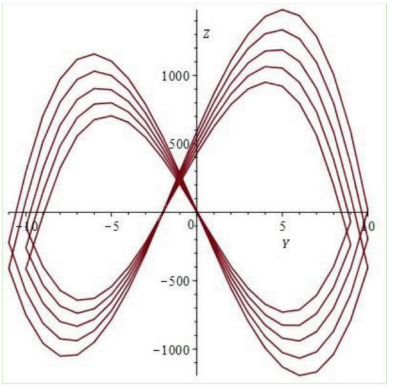

Figure 14: Figure shows the orbit of ψ which is plotted on *XY-plane*

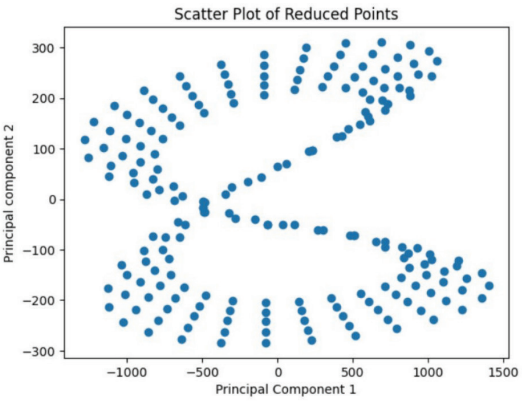

Figure 15: The figure shows PCA visualisation of ω on the *XY-plane*

findings in Figures 12 and 13, the period of the orbit of ω is periodic with period $\hat{\alpha}$. To be specific, for a start, we may choose any initial condition (X_0, Y_0, Z_0) to begin with. After some iterations under ω, the orbit of ω may become periodic and non-periodic. For periodic cases (the orbits stop iterating), then there is not a problem. However, for the non-periodic case, we have to force stop the iteration and choose any orbit points in the iteration (X_n, Y_n, Z_n) except for the initial condition (X_0, Y_0, Z_0). For example, we choose (X_1, Y_1, Z_1) as the new initial condition. By iterating the orbit of ω using the new (X_1, Y_1, Z_1), the orbit of ω becomes periodic. This result, however, needs to be further investigated for future research.

Next, we want to reduce the dimension of the map ω into a 2-dimensional space. Again, we apply the PCA method to this case to reduce the dimensionality of these 3-dimensional coordinates to 2-dimensional coordinates. We want to transform high-dimensional data into a lower-dimensional space while retaining the data's most relevant patterns or structures. After completing the PCA process using Google Colab, we obtained the following diagram.

By comparing the diagram in Figures 12 and 14, there is a similarity in the structure of map ω viewed in *XY*-plane and with the reduced plot by using PCA. Originally the map defined in (4) is a complete rotation around the origin (0,0). Now both diagrams in Figures 12 and 14 look "twisted". For both figures, the periodicity of the maps is sustained in which the orbits rotate around their centre point $\hat{\alpha}$ times. Thus, we have the following conjecture.

Conjecture 1: *Let* $\hat{\alpha} = \hat{\alpha} = x = \frac{\alpha}{gcd\,(\alpha, 2\beta)}$ *and let* ω *be the 3-dimensional map defined in (7). For some initial conditions* $(X_0, Y_0, Z_0) \in Z$, *the orbit of* ω *periodic with period* $\hat{\alpha}$.

Conclusions

Based on our findings in Case 1 and Case 2, we sustain the periodicity of the 2-dimensional map after the modification of the 2-dimensional map into a 3-dimensional map may result in the non-periodicity case. To support our claim, by modifying the 2-dimensional into 3-dimensional discrete space and then reducing it back using the PCA method, most main features of the rotation of both maps ψ and ω defined in (5) and (7) are still maintained, especially in the "twisted" case. The main result of this paper is to investigate the periodicity of the orbit of the 2-dimensional discrete Chirikov-Taylor standard map defined in (4), which can be viewed in a 3-dimensional case. Then, does the reduction from the 3-dimensional to 2-dimensional map result in a distinct structure between them? The dynamics in the 2-dimensional case could be a simple rotation around the origin. However, in the 3-dimensional case, it could be something

more interesting, as shown in Case 2. More investigation is needed in studying the behaviour of the orbit of ω as stated in **Conjecture 1**.

Acknowledgements

This research was financially supported by the Research Management Centre Grant 2020 (RMCG) Research Project RMCG20-005-0005 Entitled "Rotation On a 3-Dimensional lattice".

Conflict of Interest Statement

The authors declare that they have no conflict of interest.

References

Alwani, F., & Vivaldi, F. (2018). Nonlinear rotations on a lattice. *Journal of Difference Equations and Applications*, *24*(7), 1074-1104.

Asadi, S., Rao, C. D. V. S., & Saikrishna, V. (2010). A comparative study of face recognition with principal component analysis and cross-correlation technique. *International Journal of Computer Applications*, *10*(8), 17-21.

Bailey, S. (2014). *Building and Using a Character in 3D Space.*

Beane, A. (2012). *3D animation essentials*. John Wiley & Sons.

Chirikov, B., & Shepelyansky, D. (2008). Chirikov standard map. *Scholarpedia*, *3*(3), 3550.

Daffertshofer, A., Lamoth, C. J., Meijer, O. G., & Beek, P. J. (2004). PCA in studying coordination and variability: A tutorial. *Clinical Biomechanics*, *19*(4), 415-428.

Ghani, D. A., Supian, M. N. B., & Abdul'Alim, L. Z. B. (2019). The research of 3D modeling between visual & creativity. *International Journal of Innovative Technology and Exploring Engineering*, *8*, 180-186.

Haramburu, P., & Delrieux, C. (2006). Exploring non-linear 3D dynamical systems. In *MSV* (pp. 237-242).

Karamizadeh, S., Abdullah, S. M., Manaf, A. A., Zamani, M., & Hooman, A. (2013). An overview of principal component analysis. *Journal of Signal and Information Processing*, *4*(3B), 173.

Kurita, T. (2019). Principal component analysis (PCA). *Computer Vision: A Reference Guide*, 1-4.

Luan, X., Xie, Y., Ying, L., & Wu, L. (2008). Research and development of 3D modelling. *IJCSNS International Journal of Computer Science and Network Security*, *8*(1), 49-53.

Lucas, S. K., & Sander, E. (2022). Modeling dynamical systems for 3D printing. *The Best Writing on Mathematics 2021*, *21*, 82.

Rannou, F. (1974). Numerical study of discrete plane area-preserving mappings. *Astronomy and Astrophysics*, *31*, 289.

Remondino, F., & El-Hakim, S. (2006). Image-based 3D modelling: A review. *The Photogrammetric Record*, *21*(115), 269-291.

Zhang, X. S., & Vivaldi, F. (1998). Small perturbations of a discrete twist map. In *Annales de l'IHP Physique théorique, 68*(4), 507-523.